REPORT DOCUMENTATION PAGE

AFRL-SR-BL-TR-00-

0348

Public reporting burden for this collection of information is estimated to average 1 hour per response, including the time for review the data needed, and completing and reviewing this collection of information. Send comments regarding this burden estimate or a reducing this burden to Washington Headquarters Services, Directorate for Information Operations and Reports, 1215 Jefferson D Management and Budget, Paperwork Reduction Project (0704-0188), Washington, DC 20503

1. AGENCY USE ONLY (Leave blank)	2. REPORT DATE 6/30/2000	3. REPORT TYPE A... Final technical, 7/1/96-6/30/2000

4. TITLE AND SUBTITLE
Optical processes in semiconductor microcavities

5. FUNDING NUMBERS
F49620-96-1-0310

6. AUTHOR(S)
Hailin Wang

7. PERFORMING ORGANIZATION NAME(S) AND ADDRESS(ES)

University of Oregon
Research Service and Administration
Eugene, OR 97403-5215

8. PERFORMING ORGANIZATION REPORT NUMBER

9. SPONSORING / MONITORING AGENCY NAME(S) AND ADDRESS(ES)

AFOSR/NE
801 North Randolph St.
Room 732
Arlington, VA 22203-1977

10. SPONSORING / MONITORING AGENCY REPORT NUMBER

11. SUPPLEMENTARY NOTES

12a. DISTRIBUTION / AVAILABILITY STATEMENT

Approved for public release,
distribution unlimited

12b. DISTRIBUTION CODE

13. ABSTRACT *(Maximum 200 Words)*

The final technical report for grant F49620-96-10310 summarizes research performed on optical processes in semiconductor microcavities. This research program has lead to new understanding on nonlinear optical processes in the nonperturbative regime in semiconductor microcavities and to the development of a novel microcavity that can combine extreme photonic confinement in fused silica microspheres with electronic confinement in semiconductor nanostructures.

20000804 201

14. SUBJECT TERMS
semiconductor microcavity, normal mode oscillation
whispering gallery mode, quantum well, quantum dot, cavity QED

15. NUMBER OF PAGES

16. PRICE CODE

17. SECURITY CLASSIFICATION OF REPORT	18. SECURITY CLASSIFICATION OF THIS PAGE	19. SECURITY CLASSIFICATION OF ABSTRACT	20. LIMITATION OF ABSTRACT
unclassified	unclassified	unclassified	

Final Technical Report

Optical Processes in Semiconductor Microcavities

F49620-96-1-0310

Project Title: Optical Processes in Semiconductor Microcavities

Principal Investigator: Hailin Wang
Assistant Professor
Department of Physics
University of Oregon
Eugene, OR 97403
voice 541-346-4758
fax 541-346-4315
hailin@oregon.uoregon.edu

Institution: University of Oregon
Research Service and Administration
Eugene, OR 97403-5215

Grant Number: F49620-96-1-0310

Reporting Period: July 1, 1996 through June 30, 2000

DTIC QUALITY INSPECTED 4

1. OVERVIEW

Our program on optical processes in semiconductor microcavities has focused on two areas: i) understanding nonlinear optical processes in the nonperturbative regime in semiconductor microcavities and ii) developing a novel microcavity that can combine extreme photonic confinement in fused silica microspheres with electronic confinement in semiconductor nanostructures.

We have carried out extensive experimental and theoretical studies on coherent nonlinear optical processes in planar semiconductor microcavities and have achieved considerable new understanding on the manifestation of coherent nonlinear optical processes in the nonperturbative regime [1-4]. We show that coherent oscillations in transient four wave mixing (FWM) do not correspond to normal model oscillation (NMO) in either exciton or photon population as previously believed. These oscillations are the result of interference between different nonlinear optical processes including band filling and exciton manybody interactions. We have also developed a theoretical model to describe coherent nonlinear optical processes in the nonperturbative regime.

We have investigated biexcitonic effects in semiconductor microcavities [7]. Using polarization-dependent transient pump-probe techniques, we show that biexcitonic effects play an important role in nonlinear optical response in the nonperturbative regime. Biexcitonic interactions can lead to a significant increase in normal mode splitting (NMS) between polariton modes, in contrast to other nonlinear optical processes such as band filling that reduces NMS. Theoretical models based on a phenomenological four level system also predict new coupled excitations associated with the exciton to biexciton transition when the biexciton binding energy is large compared with both the exciton and cavity linewidth.

We have developed composite systems that combine an epitaxially-grown semiconductor quantum well (QW) or quantum dot (QD) sample with a fused silica microsphere by placing the sample in the evanescent field of the microsphere and have used various spectroscopic techniques based on frustrated total internal reflection to characterize these composite systems. We show that Q-factors of the composite system approach 10^6 and that excitonic emissions from the QW or QD sample couple efficiently into whispering gallery modes (WGMs) of the microsphere [5, 6, 8]. In addition, we have also developed a composite microsphere-nanocrystal system by spin-coating the surface of a silica microsphere with ZnS-capped CdSe nanocrystals. We show that Q-factors of the composite microsphere-nanocrystal system exceed 10^8. This composite nanocrystal-microsphere system opens up a new avenue for quantum optics studies at the mesoscopic level of a single QD. The composite system also provides us a promising candidate for deterministic generation of quantum entanglement of QDs through exchange of cavity photons between different QDs, as we have proposed and analyzed [9].

In this final technical report, we will describe in detail the significant work accomplished in our research program. Publication and education activities supported by the program will also be summarized. (Reference numbers cited above refer to papers in the publication list.)

2. ACCOMPLISHEMNT/NEWFINDINGS

2.1 Coherent oscillations in semiconductor microcavities

Nonlinear optical spectroscopy such as FWM has provided a powerful tool for probing coherent optical interactions in semiconductors. Transient FWM studies carried out in our program have led to new understanding on coherent nonlinear optical processes in the nonperturbative regime, especially, on coherent oscillations and manifestation of exciton-exciton interactions in FWM.

a) Experiment

In self-diffracted transient FWM, two laser pulses, incident at times t_1 and t_2 and with wave vectors $\mathbf{k}_1$ and $\mathbf{k}_2$, interact in a sample, generating FWM signals along directions of $2\mathbf{k}_2-\mathbf{k}_1$ and $2\mathbf{k}_1-\mathbf{k}_2$. For our study, FWM signal along the direction of $2\mathbf{k}_2-\mathbf{k}_1$ is detected in a reflection geometry. The incident laser pulses are centered between two cavity-polariton resonances and have a duration of 150 fs. The sample consists of four 13 nm $GaAs/Al_{0.3}Ga_{0.7}As$ QWs placed at the center (anti-node) of a λ cavity. The heavy hole (hh) exciton absorption linewidth is 1 nm and the minimum normal mode splitting is 2.6 nm. All measurements were performed at 10 K.

Figure 1 shows time-integrated FWM response as a function of $\tau=t_2-t_1$ at given polariton modes. Figure 1a is obtained at zero exciton-cavity detuning. Figure 1b is obtained when the cavity mode is tuned to 3 nm below the hh exciton line center. The $\tau=0$ position is determined accurately by using the symmetry property of FWM with respect to τ for signals along directions of $2\mathbf{k}_2-\mathbf{k}_1$ and $2\mathbf{k}_1-\mathbf{k}_2$, as shown in the inset of Fig. 1a. Incident photon flux used for the above measurements is of order $5\text{x}10^{11}$/pulse/cm^2. Qualitative behavior of FWM responses is independent of the excitation level in the range of photon flux (10^{10} to 10^{12}/pulse/cm^2) we have used. In addition, co-circularly polarized laser pulses were used to avoid biexcitonic effects.

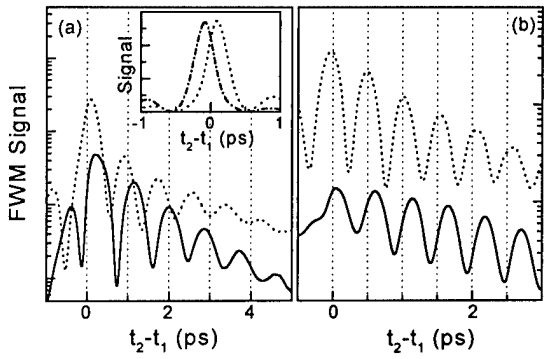

Fig. 1 Time-integrated FWM response for the upper (solid lines) and lower (dashed lines) cavity-polariton modes. (a) At zero exciton cavity detuning. (b) The cavity mode is 3 nm below the hh exciton line center. The inset in (a) also shows FWM responses near t_2-t_1=0 along the directions of $2\mathbf{k}_2-\mathbf{k}_1$ (dashed lines) and $2\mathbf{k}_1-\mathbf{k}_2$ (dotted lines) for the lower cavity-polariton mode.

Figure 2 plots node positions of oscillations in Fig. 1. The node positions form a straight line. The slope of the line determines the frequency of the oscillation. The intercept of the line at $\tau=0$ determines the initial phase of the oscillation. These results show that oscillations in Fig. 1 are $\cos^2(\Delta\tau+\theta)$-like where 2Δ is the normal mode splitting. The phase shift θ, which is given in Fig. 2, differs for the two polariton modes and depends on the exciton-cavity detuning.

For the lower polariton mode, especially when the cavity resonance is tuned below the exciton line center, $\theta \approx 0$ and the oscillation in FWM is $\cos^2(\Delta\tau)$-like.

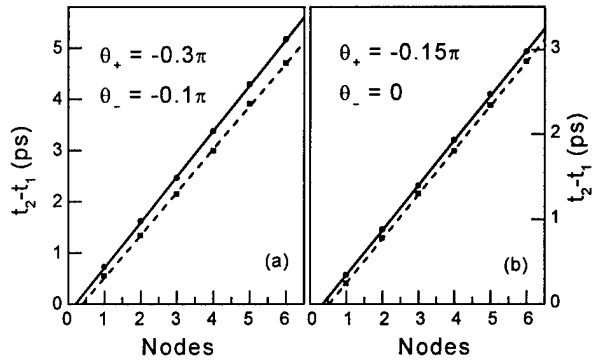

Fig. 2 Node positions of oscillations shown in Fig. 1. Circles and squares are for upper and lower cavity-polariton modes, respectively. $\theta_{\pm}$ is the initial phase of the oscillation for the upper and lower polariton modes as discussed in the text.

The observation of the nearly $\cos^2(\Delta\tau)$-like FWM response is surprising. It is believed that in self-diffracted FWM, optical polarization induced by the first pulse determines coherent dynamics of time-integrated FWM at a given polariton mode. In the nonperturbative regime, the intensity of optical polarization and the corresponding exciton population feature a $\sin^2(\Delta\tau)$-like oscillation after an impulsive excitation of the cavity mode. A $\sin^2(\Delta\tau)$-like oscillation is thus expected for FWM responses at both polariton modes. Our results clearly show that the coherent oscillations observed in transient FWM do not correspond to normal model oscillation in either exciton or photon population as previously believed.

b) Theory

To describe coherent nonlinear optical processes in the nonperturbative regime, we have developed a theoretical model based on Maxwell's equations and modified optical Bloch equations of semiconductors.

In the nonperturbative regime, coherent dipole coupling between the exciton and the cavity mode needs to be considered to all orders. To treat this dipole coupling nonperturbatively, we define two coupled optical excitations $\beta_{\pm} = \alpha \pm iC_{\pm}p$, where p is proportional to the optical polarization, α is proportional to the optical field at the position of the QW, and $C_{\pm}$ is a mixing parameter that depends on exciton-cavity detuning, relevant linewidth, and the collective dipole coupling rate Ω. $C_{\pm} = 1$ if the exciton and the cavity mode are on resonance and of equal linewidth. Under resonant optical excitation, the equation of motion for $\beta_{\pm}$ (written in the rotating frame of an external field at ω centered between the exciton and the cavity resonance) is given by

$$\dot{\beta}_{\pm} = -(\pm i\Delta + \gamma_{\pm})\beta_{\pm} + e(t) \pm iC_{\pm}(S_{+}\beta_{+} + S_{-}\beta_{-})N/N_0, \qquad (1)$$

where 2Δ is the normal mode splitting, N is the exciton population near K=0 and N_0 is the saturation exciton population, $e(t)$ is the normalized external field, and $\gamma_{\pm}$ is the polariton dephasing rate. In the weak excitation limit, $\beta_{\pm}$ corresponds to the excitation (unnormalized) of

two polariton modes. In the nonlinear regime, interactions between polaritons and the resulting nonlinear optical process can be considered as arising from intra-mode or inter-mode scattering of polaritons with the scatting amplitude proportional to

$$S_{\pm} = [2C_{\mp}\Omega \pm (2\varepsilon + i\sigma N_0)]/(C_+ + C_-), \qquad (2)$$

where ε is the static Lorentz local field correction due to renormalized electric field, and σN represents an increase in the exciton dephasing rate due to excitation induced dephasing (EID). $S_{\pm}$ includes contributions to nonlinear optical response from band filling and effects of exciton manybody interactions such as EID and local field effects. The nonlinear term in Eq. 1 is proportional to $C_{\pm}$ since interactions between polaritons take place via underlying interactions between excitons. Equation 1 along with the equation of motion for the exciton population near K=0

$$\dot{N} = -\Gamma N - \Omega(\alpha^* p + \alpha p^*), \qquad (3)$$

where Γ is the population decay rate of excitons near K=0, describes most of resonant linear and nonlinear optical processes in the strong coupling regime. Note that biexcitonic effects are ignored in the above model. Biexcitonic effects, which have also been shown in our studies to play an important role in nonlinear optical processes as we discuss in the next subsection, can be avoided in transient FWM by using co-circularly polarized laser pulses.

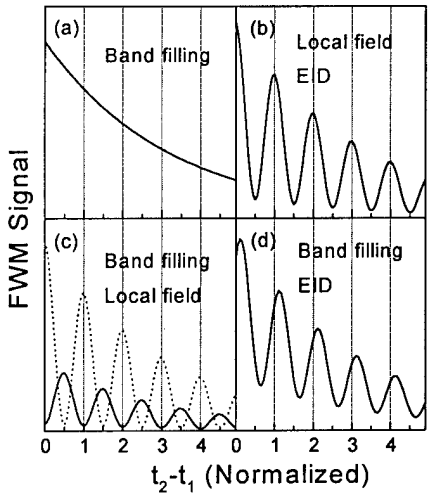

Fig. 3 Calculated time-integrated FWM response due to mechanisms indicated in the figure where we have assumed that the cavity is resonant with the exciton and have also assumed $\varepsilon/\Omega = -0.5$, $\sigma N_0/\Omega = 0.8$, $\gamma/\Omega = 0.05$, and Ω=2.5 meV. The time delay is normalized to the oscillation period. Except for (c), FWM responses are identical for both cavity-polariton modes. For (c), the solid (dashed) line is for the upper (lower) cavity-polariton mode.

To illustrate how transient FWM depends on details of exciton-exciton interactions involved, we show in Fig. 3 calculated self-diffracted FWM response when a given or a combination of nonlinear mechanisms are involved. For simplicity, we assume an impulsive external excitation and take the exciton and the cavity mode to be on resonance and of equal linewidth. As shown in Fig. 3, when FWM arises entirely from band filling, the time-integrated FWM response contains no oscillation. Pronounced coherent oscillations take place when we include contributions of exciton manybody interactions. The temporal behavior of these oscillations depends sensitively on the relative contribution of various effects of exciton-exciton interactions. Figure 3c also shows that nonlinear responses of upper and lower polariton modes

differ significantly even when the exciton and cavity are on resonance and of equal linewidth. This difference reflects the fact that band filling and local field effects interfere destructively for the upper polariton mode but constructively for the lower polariton mode.

Figure 4 shows time-integrated FWM where $\varepsilon/\Omega = -0.5$ and $\sigma N_0/\Omega = 0.8$ are used. Contributions from both EID and local field effects are necessary in order to reproduce qualitatively the phase of the oscillations shown in Fig. 2. These results show that coherent oscillations observed in transient FWM provide a "fingerprint" for the underlying exciton-exciton or polariton-polariton interactions.

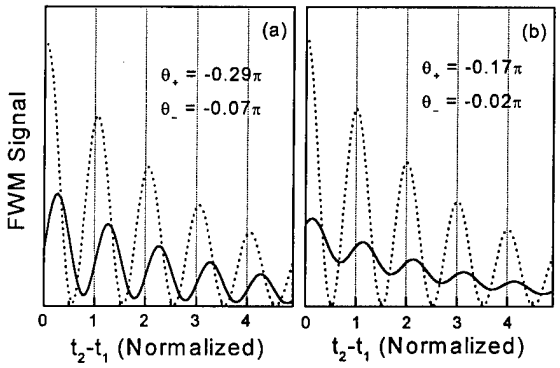

Fig. 4 Calculated time-integrated FWM response for the upper (solid lines) and lower (dashed lines) cavity-polariton modes. Nonlinear processes including band filling, local field, and EID are included. The time delay is normalized to the oscillation period. (a) δ=0. (b) δ=1.

c) Laser emission from cavity polaritons

In an effort to investigate effects of normal mode oscillation on lasing processes, we have demonstrated that laser emission can occur in a regime where cavity-polaritons or coupled exciton-cavity modes still persist [3]. We have shown that lasing threshold decreases drastically when the cavity resonance is tuned to the low energy tail of an inhomogeneously broadened exciton distribution. The minimum threshold density is obtained at a few meV below the exciton absorption line center and is considerably below the exciton saturation density. Laser emission in this regime arises from population inversion of localized excitons in the QW and the extremely small threshold is due to the fact that the number of localization sites is small at the tail of the inhomogeneous distribution. An abrupt increase in the lasing threshold is also revealed when the excitonic system undergoes the Mott transition or when cavity-polaritons vanish.

While the above results do not directly suggest effects of normal mode oscillation in the lasing process, demonstration of population inversion of an excitonic system in a high Q-cavity provides us a stepping stone for future studies of possible contributions from superradiant emission and roles of normal mode oscillation in the laser emission. Note that earlier studies in atomic systems have shown that for an initially inverted atomic system in a resonant high Q-cavity, collective interactions between the atomic system and the cavity can lead to a macroscopic polarization through a superradiant process and can result in normal mode oscillations in the superradiant emission.

During the course of above study, we have also resolved a major issue with regard to condensation of cavity-polaritons in semiconductor microcavities [2]. By comparing directly reflection and emission spectra near the lasing threshold of semiconductor microcavities, we have shown that when the cavity is near the exciton absorption line center, cavity-polaritons vanish at an excitation level far below the lasing threshold and previous claims of condensation of cavity polaritons are erroneous.

2.2) Biexcitonic effects in semiconductor microcavities

Excitonic molecules or biexcitons also play an important role in nonlinear optical interactions in semiconductor microcavities. Using polarization-dependent transient pump-probe spectroscopy, we show that biexcitonic effects can result in a significant *increase* in normal mode splitting (NMS) of cavity-polaritons, in sharp contrast to effects of band-filling and exciton ionization that reduce the NMS. A theoretical model based on modified optical Bloch equations has also been developed to describe qualitatively effects of biexcitons in semiconductor microcavities.

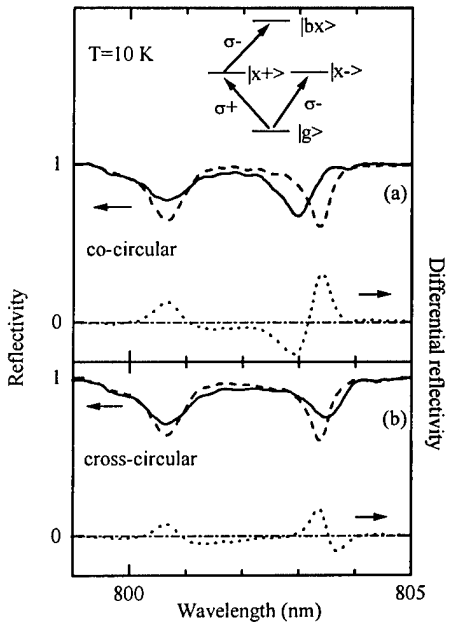

Fig. 5 Pump-probe reflection spectra. The dashed lines show as a reference spectra obtained in the absence of the pump beam. The solid lines are obtained when the sample is pre-excited with a resonant pump beam. The dotted lines represent the corresponding differential spectra. The pump and probe beams have the same and opposite circular polarization for (a) and (b), respectively. The inset shows the energy level structure used to model the biexcitonic contribution. The delay between the pump and probe pulses is less than 1 ps.

Reflection spectra of the microcavity when the sample is pre-excited by a resonant pump pulse are shown in Fig. 5. A significant increase in the NMS occurs when the pump and probe pulses have the opposite circular polarization. In comparison, when the pump and probe pulses have the same circular polarization, a reduction in the NMS occurs. The observation of an increase in NMS is quite surprising since earlier pump-probe studies have all shown a decrease in NMS along with linewidth broadening of cavity-polaritons. In addition, an increase in NMS also corresponds to enhancement rather than bleaching of the relevant absorption process.

The unique polarization dependence of the reflection spectra shown in Fig. 5 indicates that biexcitonic effects play an essential role. The magnitude of NMS in semiconductor microcavities is determined by the overall oscillator strength of the relevant optical transition. When the microcavity structure is resonantly excited by a σ+ polarized pulse, NMS of cavity-polaritons associated with the σ+ excitonic transition decreases due to absorption saturation. NMS for cavity-polaritons associated with the σ- transition, however, can behave very differently. The presence of the σ+ excitons does not lead to band-filling for the σ- excitonic transition. In addition, since biexcitons can be formed from excitons with opposite spins, the induced exciton-to-biexciton transition can lead to an increase in the overall oscillator strength for the σ- transition and subsequently an increase in the NMS provided that the biexciton binding energy is small compared with or comparable to the inhomogeneous linewidth of the excitons (for GaAs QWs the biexciton binding energy is of order 1 to 2 meV).

To describe qualitatively effects of biexcitons in semiconductor microcavities, we have developed a theoretical model based on the coupled oscillator approach and modified optical Bloch equations. The effects of bound biexcitonic states are included by using a four level system shown in the inset of Fig. 5. In addition to an increase in NMS due to the exciton-to-biexciton transition, the model also shows that the induced energy shift for the lower-branch cavity-polariton is much greater than that for the upper branch cavity-polariton (see Fig. 6), in agreement with the experimental observation.

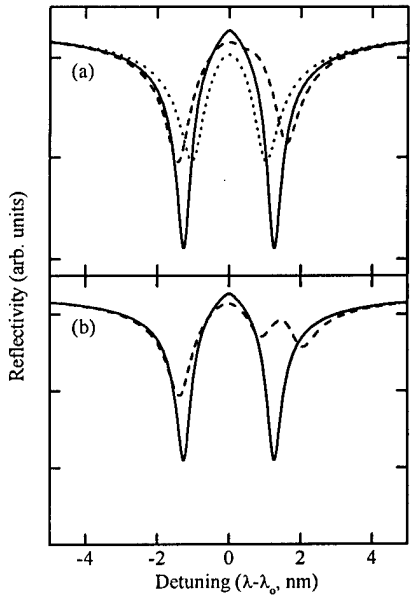

Fig. 6 Reflection spectra calculated based on the model discussed in the text. The solid lines show the reflection spectra in the low excitation limit. The dotted and dashed lines are reflection spectra at a given density of σ+ excitons and are for σ+ and σ- polarized probes, respectively. The biexciton binding energy is assumed to be 1.2 meV in (a) and 3 meV in (b).

In the limit that the biexciton binding energy is large compared with the exciton and cavity linewidth, new coupled excitations can arise from a strong coupling between the cavity mode and the exciton-to-biexciton transition. As a result, an additional cavity-polariton resonance can emerge in the reflection spectrum as shown in Fig. 6b where we have used a biexciton binding energy of 3 meV. It should be noted that in this case the strong coupling

between the cavity mode and the exciton-to-biexciton transition affects strongly all cavity-polariton resonances.

2.3) Combined semiconductor-microsphere system

Dielectric microspheres are unique and versatile optical microresonators. In a dielectric microsphere, whispering gallery modes (WGMs) form via total internal reflection along the curved boundary. Slight deformation of the sphere also removes azimuthal degeneracy of the WGMs. Lowest order WGMs are thus a ring along the equator of the sphere and are confined within a wavelength of the sphere surface, as shown schematically in Fig. 7. These WGMs can feature ultrahigh Q-factors and extremely small mode volume. Both parameters are critical for achieving strong light-matter coupling in an optical resonator and for achieving ultra-low lasing threshold. For fused silica microspheres, Q factors can exceed 10^9. Maximum vacuum field strength, $E_{vac} = \sqrt{\hbar\omega / \varepsilon_0 V}$, where V is the mode volume, can exceed 100 V/cm (λ=800 nm) for a sphere with a diameter of 20 μm. Extensive research efforts have aimed at taking advantage of these unique properties of silica microspheres for cavity QED studies of atoms, molecules, and semiconductors, and for applications in microlasers and nonlinear optics.

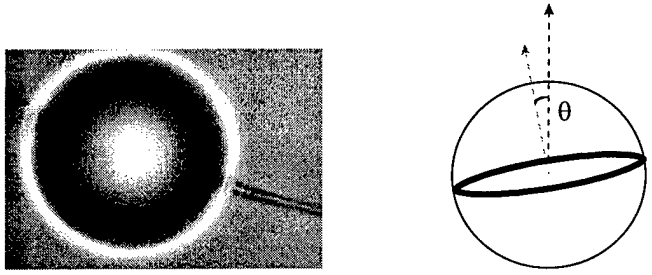

Fig. 7 A silica microsphere attached to a fiber stem and schematics of a WGM circling around the perimeter. Note that the mode volume is much smaller than the volume of the sphere.

We have fabricated silica microspheres by fusing the tip of a tapered optical fiber. The size of the sphere can range from 10 μm to more than 200 μm in diameter. The spheres are slightly elliptical and the ellipticity can be varied by heating the fiber tip asymmetrically. Figure 7 shows a 115 μm diameter sphere attached to a small fiber stem. Figure 8a shows the resonant scattering spectrum of a 140 μm diameter sphere where we have used a high index prism to couple external fields into the WGMs via frustrated total internal reflection. The free spectral range (FSR) of the WGMs is 10 Å and is determined by $\lambda^2 / \pi n D$ where λ, n, and D are the wavelength in vacuum, index of refraction (n=1.452), and the diameter of the sphere, respectively. The two peaks within one FSR shown in Fig. 2a correspond to WGMs with different radial mode numbers, i.e., WGMs with different radial distributions. Each peak in Fig. 8a also contains a number of much sharper resonances as shown in Fig. 8b. These resonances correspond to WGMs that have different azimuthal mode number or different inclination angle θ shown in Fig. 7. The removal of azimuthal degeneracy provides a convenient mechanism to select a single WGM.

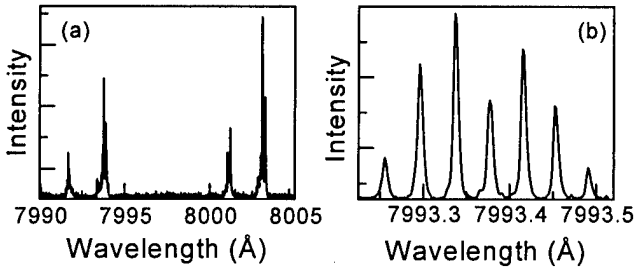

Fig. 8 Mode structure of a 140 μm diameter microsphere. (b) is an expanded plot of a peak in (a).

The spectral linewidth of the WGM resonance shown in Fig. 8b corresponds to a Q-factor of 10^6 and is limited by the output coupling loss through the high index prism used in the measurement. Much higher Q-factors are obtained when we introduce a small gap between the sphere and prism. The spectral linewidth shown in Fig. 9 corresponds to a Q-factor approaching 10^8 and is limited by the spectral linewidth of the laser used in this measurement.

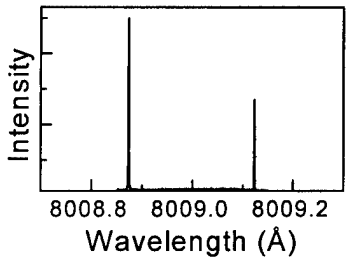

Fig. 9 High-Q WGMs measured with a small gap between the sphere and the high index prism. The spectral linewidth is of order 0.0001 Å.

In its simplest geometry, the composite microsphere-semiconductor system we have developed consisted of a microsphere in contact with a QW or QD sample, as shown in Fig. 10. We also placed a high index prism on the other side of the microsphere for output coupling of WGMs. The gap between the sphere and the prism can be adjusted by using a piezoelectric translation stage. The composite system can be excited by launching WGMs on the equator of the sphere via frustrated total internal reflection from the prism and can also be excited by creating directly electron-hole pairs or excitons in the QW sample. Photoluminescence (PL) that is coupled into the WGMs (coupled PL) and conventional PL (uncoupled PL) are along different directions since WGMs are formed through total internal reflection inside the sphere.

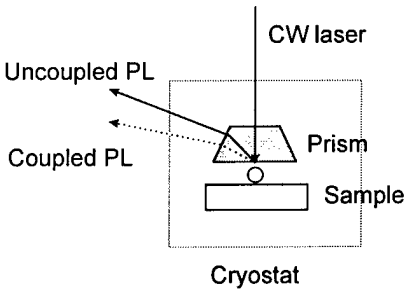

Fig. 10 Schematics for experimental setup of a composite microsphere-semiconductor system. The gap between the sphere and prism is controlled by a piezoelectric translation stage (not shown).

A number of samples have been used in our experiment, including GaAs QWs of various well thickness and exciton linewidth and QDs embedded in narrow GaAs QWs. Figure 11 shows both coupled and uncoupled PL spectra at 10 K where the QW sample with a well width of 13 nm is excited by a CW laser above the bandgap. To illustrate the mode structure of the composite system, we have chosen a sample with a large inhomogeneous linewidth. The coupled PL shown in Fig. 11b features a mode structure similar to that shown in Fig. 8a and indicates efficient coupling of PL into the WGMs of the sphere. Each peak in Fig. 11b also contains a number of much sharper WGM resonances, as shown in Fig. 11c obtained with much higher spectral resolution. The spectral linewidth of each WGM resonance is 0.1 Å and is limited by the spectral resolution of our measurement.

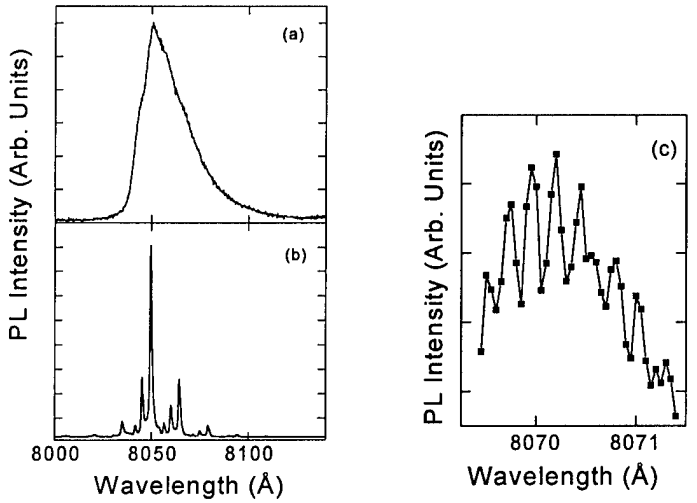

Fig. 11 Uncoupled (a) and coupled (b and c) PL spectra from a composite microsphere-QW system.

To achieve adequate spectral resolution, we have used a tunable diode laser to resonantly excite WGMs of the composite system. Figure 12 show WGM resonances in the absence and presence of the QW sample. The spectral linewidth of WGMs in the absence of the sample is 0.003 Å, corresponding to a Q-factor of 2.6×10^6, and is limited by the output coupling loss through the prism. In comparison, when the sample is placed in contact with the sphere, the linewidth of the WGMs increases to 0.018 Å, corresponding to a Q-factor of 4.4×10^5. The Q-spoiling results from output coupling loss occurring in the contact area between the sample and the sphere since the sample has an index of refraction greater than that of the silica sphere. The observed Q-spoiling agrees with our theoretical expectation. In spite of the Q-spoiling, the combined microsphere-semiconductor system still features a Q-factor significantly greater than that of monolithic semiconductor microcavities.

We have not been able to achieve laser emission or strong exciton-photon coupling using composite systems based on epitaxially-grown nanostructures. A detailed theoretical analysis has indicated that the dipole coupling rate between excitons and resonant WGMs is too small even for a homogeneously broadened QW when the sample is placed in the evanescent tail of the WGMs. While we have attempted to etch off most of the cap layer to place the QW right at the surface of the sphere, we found that for GaAs QWs and QDs, a cap layer with a minimum

thickness of 20 to 40 nm is necessary in order to avoid severe surface effects and nonradiative processes.

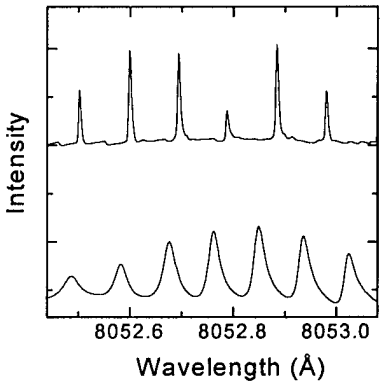

Fig. 12 WGM resonances in the absence (top curve) and presence (bottom curve) of a QW sample.

To overcome the difficulty discussed above, we have developed a microcavity system by coupling semiconductor nanocrystals to a fused silica microsphere. Nearly defect free CdSe nanocrystals have been synthesized by using organometallic synthesis. The diameter of these nanocrystals ranges from 1 to 8 nm. Efficient surface passivation has been achieved recently by encasing or capping the nanocrystals with a thin shell (~1 nm) of ZnS that has a bandgap greater than CdSe. The ZnS capping leads to a remarkably high quantum efficiency (as high as near unity) at room temperature. Figure 13 shows the experimental results obtained from a composite microsphere-nanocrystal system. The CdSe nanocrystals were fabricated in the laboratory of Professor Lonergan at the University of Oregon. Figure 13a shows a portion of the coupled PL spectrum obtained at room temperature. To determine whether coating of nanocrystals leads to significant Q-spoiling, we carried out resonant scattering studies at energies below the band gap of the CdSe nanocrystal. The spectral linewidth of 0.001 Å shown in Fig. 13b is limited by the scanning stepsize of the diode laser used for this experiment and corresponds to a Q-factor approaching 10^7. Further studies using time domain ring down spectroscopy has shown that the Q-factor of the combined nanocrystal-microsphere system can exceed 10^8.

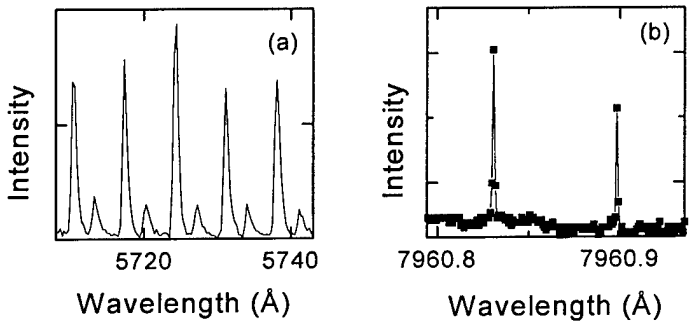

Fig. 13 Preliminary results from a composite microsphere-nanocrystal system. (a) PL spectrum reflects mode structure of the composite system. (b) Resonant scattering spectrum below the CdSe bandgap shows a spectral linewidth of 0.001 Å, corresponding to a Q-factor approaching 10^7.

The extremely high Q-factor, along with the very small effective mode volume, of the composite nanocrystal-microsphere system opens up a new avenue for exploring light-matter interactions at the mesoscopic level of a single QD. For example, the system can be used to investigate lasers of a single QD, where thermodynamic limit is no longer valid, and cavity QED of a single QD, where individual quantum transitions in a QD can strongly affect the dynamics of the system. The combined QD-microsphere system also provides us a promising candidate for deterministic generation of quantum entanglement of an array of QDs through exchange of cavity photons between different QDs, as we have proposed and analyzed recently.

In addition to cavity Q-factor and cavity mode volume, another key parameter for the cavity QED or quantum entanglement of QDs is dephasing rates in a QD. We have investigated both dephasing and population relaxation of excitons localized in QD-like islands in narrow GaAs QWs by using stimulated photon echoes. A direct comparison of these two closely related decay processes reveals a pure dephasing process that does not involve exciton population relaxation. The pure dephasing process is shown to arise from adiabatic mixing of electronic states with continuum states of acoustic phonons and is a direct result of electronic quantum confinement. At relatively high temperature (>30 K), this pure dephasing process becomes the dominant dephasing mechanism. The observed temperature dependence of the pure dephasing rate also points to qualitative differences in excitonic dephasing for semiconductors with weak and strong 3D quantum confinement. Both the magnitude and the temperature dependence of the pure dephasing rates are satisfactorily described by a theoretical model based on the Huang-Rhys theory of *F*-centers.

For QDs, energy quantization due to the 3D confinement can suppress energy or population relaxation. What we have shown is that the quantization or confinement does not suppress pure dephasing processes that do not involve electronic population relaxation and on the contrary leads to stronger pure dephasing. The fundamental understanding of dephasing achieved in our study is important for cavity QED studies in semiconductors as well as for a variety of optical processes including quantum computing that depends on optical coherence.

3. PUBLICATIONS

1. Hailin Wang, Y.-T. Chough, S.E. Palmer, and H. Carmichael, "*Normal mode oscillation in the presence of inhomogeneous broadening*," Optics Express **1**, pp370-373 (1997).
2. Xudong Fan, Hailin Wang, H.Q. Hou, and B.E. Hammons, "*Laser emission from semiconductor microcavities: the role of cavity-polaritons*," Phys. Rev. A**56**, pp3233-3236 (1997).
3. Xudong Fan, Hailin Wang, H.Q. Hou, and B.E. Hammons, "*Laser emission from semiconductor microcavities: transition from nonperturbative to perturbative regimes*," Phys. Rev. B**56**, pp15256-15300 (1997).
4. Hailin Wang, H.Q. Hou, and B.E. Hammons, "*Coherent dynamics of excitonic nonlinear optical response in the nonperturbative regime*," Phys. Rev. Lett. **81**, pp3255-3258 (1998).
5. Xudong Fan, Andrew Doran, and Hailin Wang, "*High-Q whispering gallery modes from a composite system of GaAs quantum well and fused silica microsphere*," Appl. Phys. Lett. **73**, pp3190-3192 (1998).
6. Xudong Fan, T. Takagahara, J.E. Cunningham, and Hailin Wang, "*Pure dephasing induced by exciton-phonon interactions in narrow GaAs quantum wells*," Solid State Comm. **108**, pp857-951 (1998).
7. Xudong Fan, Hailin Wang, H.Q. Hou, and B.E. Hammons, "*Biexcitonic effects in the nonperturbative regime of semiconductor microcavities*," Phys. Rev. B**57** Rapid Comm., pp9451-9454 (1998).
8. Xudong Fan, Scott Lacey, and Hailin Wang, "*Microcavities combining a semiconductor heterostructures with a fused silica microsphere*," Opt. Lett. **24**, pp771-773 (1999).
9. T. A. Brun and Hailin Wang, "*Coupling nanocrystals to high-Q silica microspheres: entanglement in quantum dots via photon exchange*," Phys. Rev. A**61**, pp323071-323075 (2000).

4. INTERACTIONS/TRANSITIONS

INVITED PRESENTATIONS:

Laser emission from semiconductor microcavities: effects of exciton localization, Physics of Quantum Electronics, Snowbird, Utah (1997).

Quantum optics of semiconductor microcavities, NSF/AFOSR Functional Meso-Optics Workshop, Crested Butte, Colorado (1997).

Coherent dynamics in semiconductor microcavities, Workshop on Quantum Dynamics in Systems far from Equilibrium, Santa Barbara, California (1997).

Stimulated emission from semiconductor microcavities: Toward laser emission from a few excitons, Physics and Simulation of Optoelectronic Devices VI, San Jose, California (1998).

Nonlinear optical spectroscopy in semiconductor microcavities, OSA Annual Meeting, Baltimore, Maryland (1998).

Coupling nanocrystals to a fused silica microsphere: a quantum-dot microcavity with extremely high Q-factors, NRL Workshop on Quantum Dots for Quantum Computing, Washington, DC (1999).

Coupling nanocrystals to a fused silica microsphere: towards entanglement of quantum dots, Physics of Quantum Electronics, Snow Bird, Utah (2000).

Coupling nanocrystals to a high-Q fused silica microsphere: cavity QED of quantum dots, Quantum Electronics and Laser Sciences (QELS'2000), San Francisco (2000).

Coupling nanocrystals to a fused silica microsphere: towards entanglement of quantum dots, American Chemical Society Symposium on Quantum Computing for the Next Millennium, Washington, DC (2000).

Coherent oscillations in nonlinear optical response of interacting excitons and polaritons, Materials Research Society Fall Meeting, Boston (2000).

CONTRIBUTED PRESENTATIONS WITH PUBLISHED PROCEEDINGS (REFEREED):

Xudong Fan, Hailin Wang, H. Hou, and B.E. Hammons, "*Stimulated emission from semiconductor microcavities*," Quantum Electronics and Laser Science, OSA Technical Digest, pp13 (1997).

Hailin Wang, H. Hou, and B.E. Hammons, "*Anomalous normal mode oscillation from semiconductor microcavities*," Quantum Electronics and Laser Science, OSA Technical Digest, pp12, (1997).

Xudong Fan, Hailin Wang, H. Hou, and B.E. Hammons, "*Laser emission from semiconductor microcavities: transition from nonperturbative to perturbative regimes*," International Quantum Electronics Conference, OSA Technical Digest, pp29-30 (1998).

Hailin Wang, Xudong Fan, H. Hou, and B.E. Hammons, "*Biexcitonic effects in semiconductor microcavities*," International Quantum Electronics Conference, OSA Technical Digest, pp31 (1998).

Hailin Wang, Xudong Fan, J.E. Cunningham, T. Takagahara, " *Pure dephasing induced by exciton-phonon interactions in GaAs quantum dots*," International Quantum Electronics Conference, OSA Technical Digest, San Francisco (1998).

Hailin Wang, H.Q. Hou, and B.E. Hammons, "*Coherent dynamics in semiconductor microcavities: effects of exciton-exciton interactions*," Quantum Electronics and Laser Science, OSA Technical Digest, pp27-28 (1999).

Xudong Fan, Scott Lacey, and Hailin Wang, "*High-Q whispering gallery modes from a combined system of GaAs quantum well and fused silica microsphere*," Quantum Electronics and Laser Science, OSA Technical Digest, pp29-30 (1999).

Xudong Fan, Hailin Wang, and Mark Lonergan, "*Attaching nanocrystals to a dielectric microsphere: a quantum dot microcavity with extremely high Q-factors*," Quantum Electronics and Laser Science, OSA Post Deadline Technical Digest (1999).

Hailin Wang, Phedon Palinginis, Xudong Fan, Scott Lacey, and Mark Lonergan, "*Coupling nanocrystals to a high-Q fused silica microsphere: cavity QED of quantum dots*," Quantum Electronics and Laser Science, OSA Technical Digest, pp99 (2000).

Xudong Fan, Hailin Wang, and Mark Lonergan, "*Probing radiative recombination in semiconductor nanocrystals with cavity QED*," Quantum Electronics and Laser Science, OSA Technical Digest, pp58 (2000).

5. EDUCATION ACTIVITY

Four Ph.D. students (Xudong Fan, Mark Philips, Scott Lacey, and Phedon Palinginis) had been supported by this program (supplemented by additional support from University of Oregon and from NSF). Mr. Fan is expected to graduate in Dec. 2000 for research performed under this program.

One student (Andrew Doran) has received MS degree through support of this program. In addition, this program has also made possible the involvement of one undergraduate student (Stephanie Palmer) in this laboratory.

6. HONORS AND AWARDS

National science foundation faculty early career award, 1998-2002.

7. PATENTS

None